



## Fabrication of ultra-pure gold nanoparticles capped with dodecanethiol for Schottky-diode chemical gas sensing devices

Radu Ionescu<sup>a, b, \*</sup>, Umut Cindemir<sup>b</sup>, Tesfalem Geremariam Welearegay<sup>a</sup>, Raul Calavia<sup>a</sup>, Zouhair Haddi<sup>a, 1</sup>, Zareh Topalian<sup>b</sup>, Claes-Göran Granqvist<sup>b</sup>, Eduard Llobet<sup>a</sup>

<sup>a</sup> Department of Electronics, Electrical and Automatic Engineering, Rovira i Virgili University, Tarragona 43007, Spain

<sup>b</sup> The Ångström Laboratory, Department of Engineering Sciences, Uppsala University, SE-75121 Uppsala, Sweden

### ARTICLE INFO

#### Article history:

Received 1 March 2016

Received in revised form 6 July 2016

Accepted 8 July 2016

Available online xxx

#### Keywords:

Monolayer-capped gold nanoparticles

Advanced gas deposition

Dip-coating

Schottky-diode chemical gas sensors

### ABSTRACT

Ultra-pure monolayer-capped gold nanoparticles for chemical gas sensing devices were prepared by a novel two-step process: a physical vapour deposition technique was first employed to make dispersed ultra-pure size-controlled gold nanoparticles, and this step was followed by a coating process for functionalization of the gold nanoparticles with an organic ligand, specifically dodecanethiol. X-ray photoelectron spectroscopy proved that the nano-assemblies had high purity. Chemical sensing devices based on these nano-assemblies showed Schottky-diode behaviour. We believe this is the first observation of Schottky-diodes fabricated from nanomaterials based on metallic nanoparticles. Gas sensing experiments demonstrated that these devices were suitable for detecting volatile organic compounds.

© 2016 Published by Elsevier Ltd.

### 1. Introduction

Electronic devices with exciting new possibilities for identification and quantification of single- or multi-component chemical and biological species can be developed by immobilising a nanoscale matrix of nanoparticles, provided with appropriate functional terminations, onto the surfaces of the device [1–3]. Monolayer-capped metallic nanoparticles, with nanoparticles connected by linkers of different molecular structures, possess excellent features for identification of target analytes; the capping can employ a wide variety of molecular ligands [4–6]. In these nanoscale sensing assemblies, the molecular functionalities provide sites for the sorption of guest (sensed) molecules, while the metallic nanoparticles give electrical conductivity and allow electron transport through the sensing film [7]. Only a few molecules are sufficient to change the electrical properties of the sensing elements in the electronic transducer, which hence can detect very low concentrations of analytes [1]. Moreover, monolayer-capped metallic nanoparticle-based devices are superior to the more widely studied metal oxide-based sensors in that they are well suited for room-temperature operation and therefore enable

power savings and safe operation even in highly flammable places [5].

Monolayer-capped metallic nanoparticles are generally made by conventional wet-chemistry methodology that uses a two-phase procedure combined, whenever necessary, with ligand exchange [8,9]. However, this procedure employs chemical precursors which leave traces of residual compounds [10,11].

In this study, we introduce a new technique that ensures the fabrication of ultra-pure monolayer-capped gold nanoparticles. This novel approach comprises two steps: (i) physical vapour deposition to make dispersed, ultra-pure, size-controlled, gold nanoparticles (AuNPs), and (ii) coating and functionalizing of the AuNPs with organic ligands.

### 2. Materials and methods

In the first processing step, AuNPs were prepared and deposited onto glass or silicon substrates by use of advanced gas deposition (AGD) [12]. The AGD equipment was adapted, as shown in Fig. 1, to comply with results of our previous studies on the fabrication of thin films of AuNPs [13,14]. For achieving the objective of the present study – i.e., deposition of dispersed (isolated) AuNPs – the nozzle between the evaporation (lower) and deposition (upper) chambers of the AGD equipment was removed in order to avoid the formation of compact gold films, which would otherwise have been favoured by the high speed of the particles driven by the pressure difference between the two chambers in the equipment.

For the fabrication of the AuNPs, a piece of high-purity gold (99.999%) was placed on a carbon crucible inside the evaporation chamber, and both chambers of the AGD unit were evacuated until

**Abbreviations:** AuNPs, gold nanoparticles; AGD, advanced gas deposition; SEM, scanning electron microscopy; XRD, X-ray diffraction; XPS, X-ray photoelectron spectroscopy; RH, relative humidity; LOD, limit of detection

\* Corresponding author at: Department of Electronics, Electrical and Automatic Engineering, Rovira i Virgili University, Tarragona 43007, Spain.

Email address: radu.ionescu@urv.cat (R. Ionescu)

<sup>1</sup> Present address: Laboratoire des Sciences de l'Information et des Systèmes, Aix-Marseille University, Marseille 13397, France.

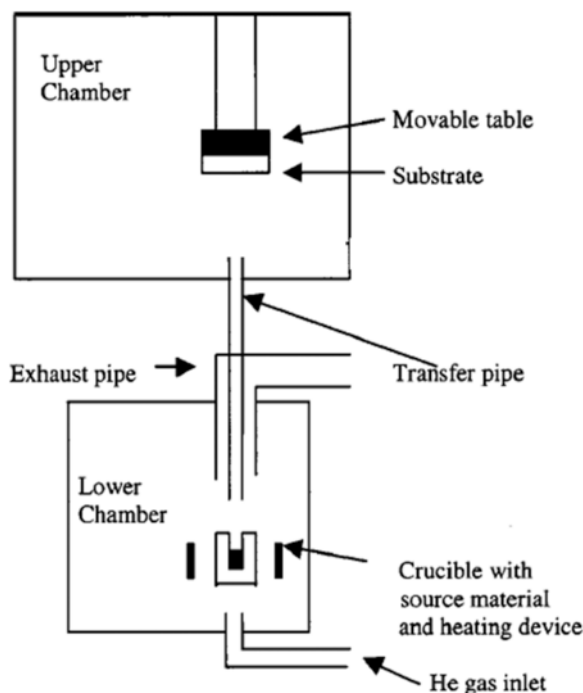


Fig. 1. Configuration of the AGD equipment employed in this study.

their pressure reached  $\sim 0.02$  mbar to ensure clean deposition conditions. A copper induction coil surrounding the crucible provided the heating necessary to melt and evaporate the gold. A laminar flow of high-purity He ( $20 \text{ l min}^{-1}$  flow rate) was introduced underneath the heated gold piece, and this gas flow, with upward direction, transported the metal vapour while cooling it down so that initially clusters of Au atoms, and subsequently single Au nanoparticles, were condensed. The pressures in the evaporation and deposition chambers were set to  $\sim 0.8$  mbar and  $\sim 88$  mbar, respectively. A transfer pipe (3 mm diameter) connecting the two chambers of the equipment, was positioned in the vapour region where the individual AuNPs were formed. Because of the pressure difference between the two AGD chambers, the gold nanoparticles were transported rapidly to the deposition chamber, thereby avoiding agglomeration. In this way, individual AuNPs with a narrow size distribution could be transferred to the upper chamber and deposited onto a substrate placed on a movable support table.

In the second processing step, the AuNPs were capped with dodecanethiol. This organic compound contains a thiol group, which is likely to bind strongly to the AuNPs because of the strong affinity of sulphur to gold [15]. The choice of dodecanethiol was founded on previous reports which showed that chemical gas sensors based on AuNPs functionalized with dodecanethiol have promising features for the detection of volatile organic compounds (VOCs) such as acetaldehyde, formaldehyde, etc. [16,17].

In order to accomplish the functionalization, we dissolved  $200 \mu\text{l}$  of dodecanethiol in ethanol. The selected solvent is conveniently volatile and evaporates quickly at low temperature; it is therefore excellent for applications that require high-purity upon evaporation [18]. Stirring for 30 min at room temperature ensured homogeneity of the solution. Samples with pre-deposited AuNPs were immersed in the solution for 1 h, and the solvent was subsequently evaporated by heating the samples at  $50^\circ\text{C}$  for 1 h in a conventional oven.

### 3. Results and discussion

The morphology of the AuNPs fabricated in the first processing step by AGD was governed by the speed of the movable support (set to its minimum value of  $0.04 \text{ mm s}^{-1}$ ) and the number of deposition cycles, as apparent from Scanning Electron Microscopy (SEM) (see Fig. 2). Thus, a single deposition cycle led to isolated gold nanoparticles (Fig. 2a). When the number of deposition cycles was increased to two, the AuNPs started to agglomerate in small clusters (Fig. 2b), while a compact thin film of AuNPs was formed when eight deposition cycles were employed (Fig. 2c).

Electrical resistance measurement between electrodes proved that no electrical contact was formed for the AuNPs samples shown in Fig. 2a and b, which hence consisted of isolated Au nanoparticles and isolated AuNPs clusters, respectively. The electrical resistance measured for the AuNPs samples shown in Fig. 2c was of the order of a few  $\Omega$ , thus indicating the formation of a continuous film of AuNPs, which is inadequate for gas sensing applications.

In order to prevent any influence from the substrate, the physical properties of the AuNPs were investigated on the film shown in Fig. 2c. The crystal orientation of the AuNPs was characterised by X-Ray Diffraction (XRD), as shown in Fig. 3. A strong diffraction peak at  $38.3^\circ$  was attributed to Au (111) planes parallel to the surface of the glass substrate. The other three diffraction peaks, attributed to Au (200) at  $44.4^\circ$ , Au (220) at  $64.8^\circ$  and Au (311) at  $77.6^\circ$ , exhibited weaker relative intensities than for Au (111). The diffraction pattern is in good agreement with that of elemental gold and shows no evidence for contamination or the formation of an any secondary gold phase. The mean crystallite size  $D$  of the AuNPs was calculated from Scherrer's formula (Eq. (1))

$$D = K\lambda / (\beta \cos \Theta), \quad (1)$$

where  $K$  is Scherrer's constant,  $\lambda$  is X-ray wavelength,  $\beta$  is peak width at half maximum, and  $\Theta$  is diffraction angle. Applying this formula to the (111) peak gives  $D \approx 11$  nm, which is in good agreement with the particle size seen from SEM images in Fig. 2a ( $\approx 10$  nm). This result ensures that the AuNPs are single crystalline. Importantly, the number of cycles used during AuNPs deposition did not have any direct influence on particle size despite the fact an increased number of deposition cycles led to AuNPs aggregation in clusters or to the formation of a thin film of AuNPs.

Functionalization of the isolated AuNPs shown in Fig. 2a with the organic ligand led to linking of the AuNPs, which aggregated into chains forming uninterrupted paths (Fig. 4). This process did not alter the size of the AuNPs, as it can be observed in Fig. 4.

Gas sensing devices were next fabricated on a 2-inch,  $p$ -type,  $10\text{--}20 \Omega$ , (100) oriented,  $275\text{-}\mu\text{m}$ -thick, single-side polished silicon wafer. A  $200\text{-nm}$ -thick  $\text{SiO}_2$  layer was first grown on top of the silicon wafer by dry thermal oxidation at  $1100^\circ\text{C}$ . Two parallel gold electrodes that are  $30 \mu\text{m}$  apart were then patterned using thin positive photoresist and laser lithography. A  $200\text{-nm}$ -thick gold film was sputtered on the  $\text{SiO}_2$  surface, and a lift-off process with acetone was finally employed for removing the gold outside the electrodes area. Fig. S1 from the Supplementary material shows the sensor layout.

Prior to the deposition of the AuNPs by AGD, the sensing devices were treated successively for 5 min in propanol and for 5 min in acetone in an ultrasound bath at room temperature. As a final step, the devices were rinsed with deionised water for removing the impurities.

The electrical resistance of the monolayer-capped AuNP sensing films shown in Fig. 4 ranged between hundreds of  $\text{k}\Omega$  to several  $\text{M}\Omega$ ,

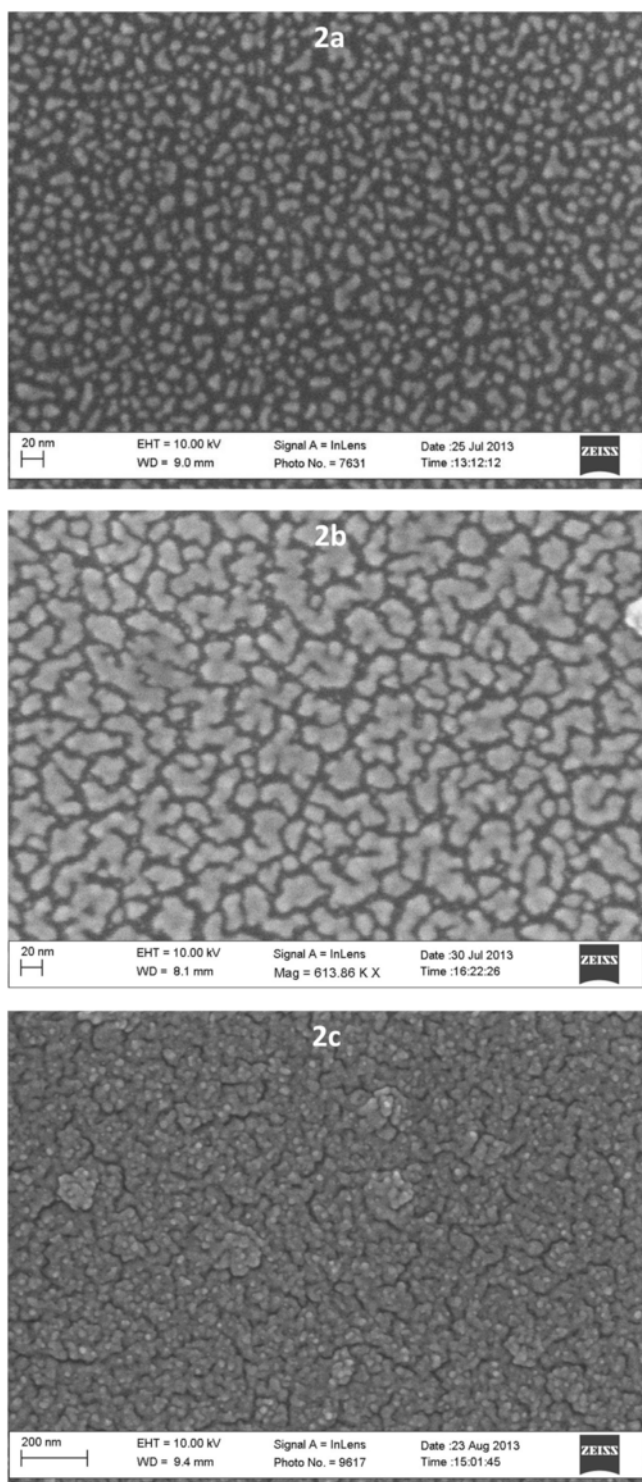


**Fig. 2.** SEM images of AuNPs deposited by AGD using different numbers of deposition cycles: (a) one; (b) two; (c) eight.

which is very suitable for gas sensing applications. An interesting phenomenon could be observed when the sample shown in Fig. 2b was functionalized with dodecanethiol. Immediately after the functionalization, the electrical resistance between the sensor electrodes was in the range of tens of M $\Omega$ . However, the nano-assembly then proved to be unstable, and the electrical resistance decreased mono-

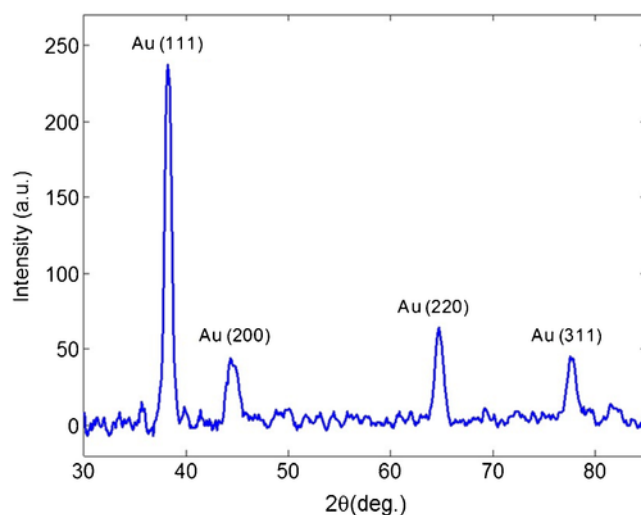


**Fig. 3.** X-ray diffractogram of the AuNPs film shown in Fig. 2c.

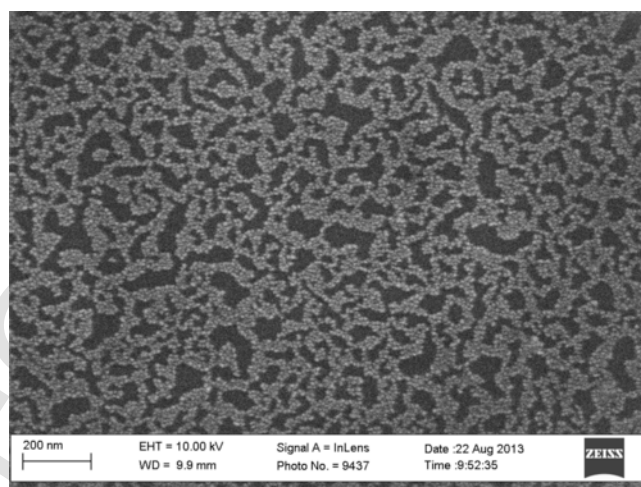


**Fig. 4.** SEM image of isolated AuNPs functionalized with dodecanethiol.

nically with time and dropped to tens of k $\Omega$  after one month. This resistance drop is believed to be due to a slow and continuous agglomeration process for the AuNPs clusters.

Based on the results reported above, we could ascertain that the best experimental methodology for the fabrication of ultra-pure monolayer-capped AuNPs nano-assemblies for gas sensing applications consisted in the deposition, in the first processing step, of isolated AuNPs onto the sensing area of the device, followed by AuNPs functionalization with the organic ligand in a subsequent step. The elemental surface composition of these samples was characterised by X-ray Photoelectron Spectroscopy (XPS) applied to the isolated AuNPs shown in Fig. 2a, before and after their functionalization with dodecanethiol (see Fig. 5). The surface composition of the samples is summarised in Table 1. A major component is Si, which indicates incomplete coverage of the substrate by the nano-assembly matrix. In addition, the Au 4f peaks were in the zero valent state, which is in concordance with previous findings [19].

Electrical characterization of the sensing devices showed Schottky diode behaviour. The electron transport through the sensing film is determined by the nano-assembly's distribution of conducting paths, and the electrical conductivity depends on the actual current injection

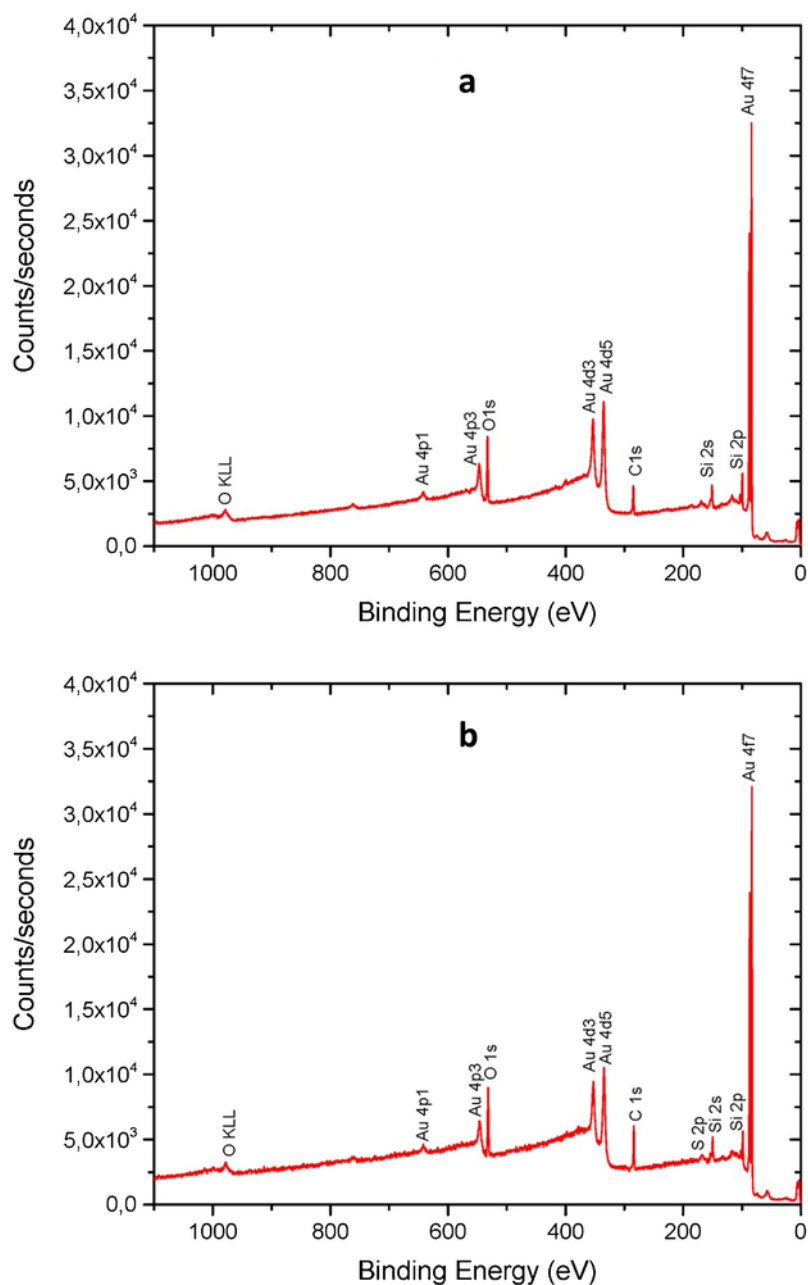


Fig. 5. XPS data of: (a) isolated AuNPs; (b) dodecanethiol-functionalized AuNPs.

**Table 1**  
Surface elemental composition of the samples analysed by XPS.

Element	Si2p	C1s	Au4f	O1s	S2p
AuNP sample	42.7%	–	29.7%	27.6%	–
Isolated AuNPs functionalised with dodecanethiol	38.4%	30.1%	13.7%	12.1%	5.6%

site that determines the positive and negative electrode, as indicated by the asymmetry of the  $I$ - $V$  characteristic (Fig. 6). The monolayer-capped AuNPs diode has a conduction threshold voltage of  $\sim 0.4$  V, which is in line with data for typical metal-weakly doped semiconductor Schottky diodes ( $\sim 0.3$  V) [20].

Gas sensing measurements were performed by exposing the Schottky-diode sensing device, placed inside a Teflon test chamber of  $\sim 4$  cm<sup>3</sup> volume, to acetaldehyde as target VOC, and ethanol and ethylbenzene as interfering species. The device was operated in direct polarisation mode, and the current between the electrodes was monitored while the applied voltage was successively swept forward and backward between zero and +10 V. The sensing measurements were performed at room temperature ( $22.5 \pm 1$  °C) and comprised successive exposure cycles to synthetic dry air (40 min) and to different concentrations of VOCs (obtained from 100% purity bottles) diluted in synthetic dry air (20 min) at a constant flow rate of 200 ml min<sup>-1</sup>. Humidity effect was investigated by introducing water vapour to the measurement gas flow by means of a glass bubbler, such that to ob-

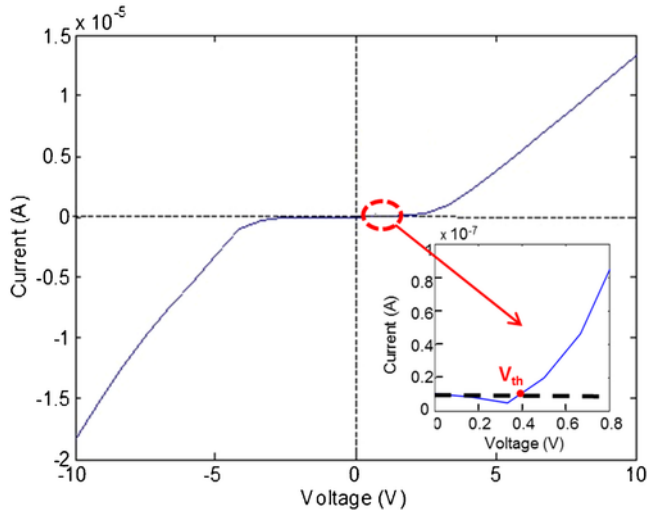


Fig. 6.  $I$ - $V$  characteristic of a monolayer-capped AuNP-based device showing Schottky-diode behaviour. The zoom shows the value of the threshold voltage.

tain at the output of the sensors chamber two different relative humidity (RH) levels (30 and 70%), covering a high RH range.

The sensor response was extracted from the  $I$ - $V$  characteristic at each voltage (see in Fig. 7, as representative example, sensor's response to 30 ppm acetaldehyde extracted at 3.33 V on the backward curve), and indicated good repeatability and recovery.

Data were taken to assess the response to the gas at several voltages and to monitor the relative current change produced by sensor's exposure to acetaldehyde in comparison with the current in synthetic dry air according to Eq. (2)

$$S^{(V)} (\%) = \frac{I_{VOC}^{(V)} - I_{air}^{(V)}}{I_{air}^{(V)}} \quad (2)$$

where  $S^{(V)}$  is the sensor's response at the voltage  $V$ ,  $I_{VOC}^{(V)}$  is the current at voltage  $V$  in the presence of the VOC, and  $I_{air}^{(V)}$  is the current at

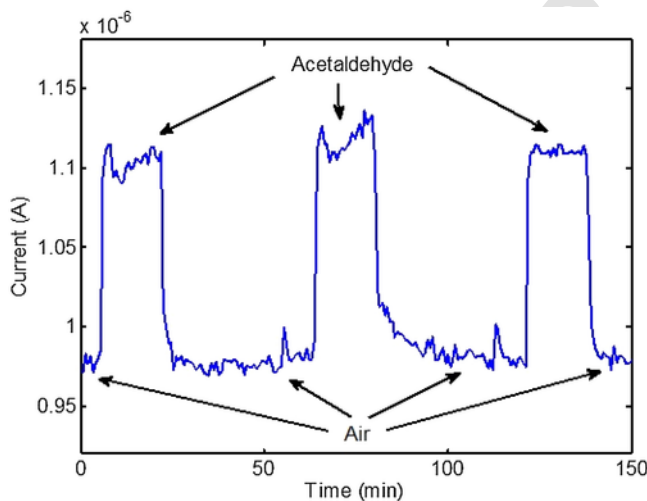


Fig. 7. Response of a Schottky-diode sensor, extracted from the sensor's  $I$ - $V$  characteristic at 3.33 V on the backward curve.

voltage  $V$  in synthetic dry air prior to VOC exposure. We used the mean value over three successive exposures to the VOC.

Fig. 8 shows the response curve obtained from exposure of the Schottky-diode sensor to 30 ppm of acetaldehyde. The diode was operated in the positive polarisation mode, with the metal (i.e., the AuNPs) at a higher potential than the organic material. By increasing the voltage, the potential barrier is decreased. As the voltage exceeds the conduction threshold voltage (0.4 V; see Fig. 6), electrons from the organic material cross over to the AuNPs. When the monolayer-capped AuNPs sensing material is exposed to acetaldehyde, there is charge exchange between the sensing material and acetaldehyde via steric interaction between the sensing film and the sensed analyte (i.e., film swelling due to analyte adsorption), which alters the charge carrier transport [1]. However, the passing over of the conduction threshold voltage does not produce an increase in the number of electrons that cross the potential barrier upon absorption of the VOC until the applied voltage reaches a sufficient value (3.33 V; see Fig. 8). Favoured by the accumulation of electrons generated by the VOC adsorbed by the sensing film, there is a sudden enhancement of the electrons' carrier transport and the sensor's response reaches its maximum value. The response is then decreasing as the capacity of the adsorbed VOC to generate new electrons is limited by the total VOC concentration. When the voltage is swept backward, the observed phenomena are opposite, with the remark that the sensor's response reaches its maximum value at a lower voltage compared with the forward characteristic (2.5 V; see Fig. 8), which is attributed to the hysteretic behaviour of the Schottky barrier height variation arising from the material's polarisation reversal [21]. By further lowering the value of the voltage applied, the potential barrier height increases over the value at which the electrons from the organic material could cross over to the AuNPs, which produces the inhibition of electrons' carrier transport through the Schottky diode device and sensor's response becomes zero.

The above results allowed determining the voltage at which the maximum response point could be obtained (3.33 V on the forward curve), which was then used to assess sensor's behaviour at a constant bias. Sensor's response to 30 ppm of acetaldehyde at a constant operation voltage of 3.33 V is shown in Fig. S2 from the Supplementary material. The response achieved in this case (13.3%) was quite sim-

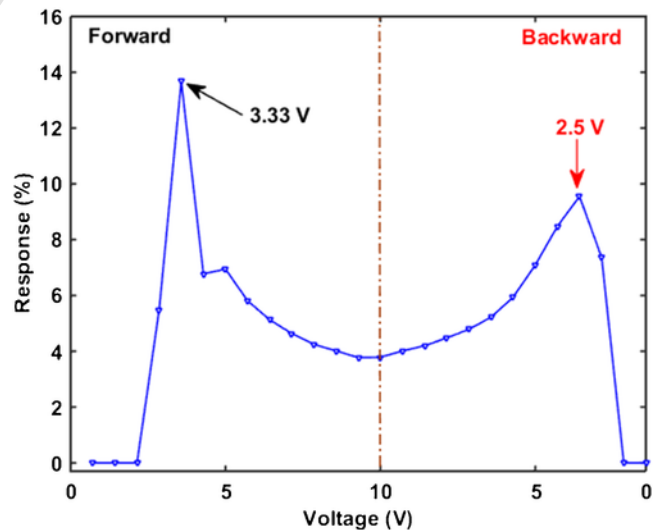


Fig. 8. Response curve obtained from an AuNP-based sensor exposed to 30 ppm of acetaldehyde.

ilar with the response extracted at the same voltage on the forward curve when the sensors was operated as a Schottky diode (13.7%).

For calculating the limit of detection (LOD) for acetaldehyde exposure, the sensor was exposed to different concentrations of acetaldehyde in the concentrations range 5–30 ppm. The calibration curve was plotted with the response values extracted at 3.33 V on the forward curve (see Fig. 9). The LOD was calculated with the formula from Eq. (3), giving a value  $LOD \approx 2.5$  ppm.

$$LOD = 3 \times Sa/b, \quad (3)$$

where  $Sa$  is the standard deviation of the y-residuals and  $b$  the slope of the regression line of the calibration curve provided in Fig. 9.

When the sensor was exposed to acetaldehyde under different humidified backgrounds, it was observed a decrease in its response under the low humidity level (30% RH), while under the high humidity level (70%) sensor's response dramatically increased (see Fig. 10). This is similar to other findings, which reported that the response of sensors based on gold-thiolate monolayer-protected nanoparticles decreases with humidity increase in the low humidity range, when the film swelling governs sensor's responses, while at high humidity the change in the dielectric properties governs the responses, which begin to reverse [22,23].

Sensor's responses to two interfering species (ethanol and ethylbenzene) showed significantly different response patterns (see Fig. 11), which indicates that the measurement technique and the novel method that we introduced in this study to analyse the response of a Schottky-diode chemical gas sensor offers novel features for fingerprinting VOC detection.

Finally, it is worth mentioning that the sensor was studied over a three years period, keeping intact its operation capabilities throughout all this period, which suggests a good robustness and a long lifetime period.

#### 4. Conclusions

This study reports the fabrication of ultra-pure, monolayer-capped, AuNPs employing a novel technique that consists of two steps: AGD is first employed to make dispersed ultra-pure, size-controlled, AuNPs, and this step is then followed by a coating process to functionalize the AuNPs with dodecanethiol. Chemical gas

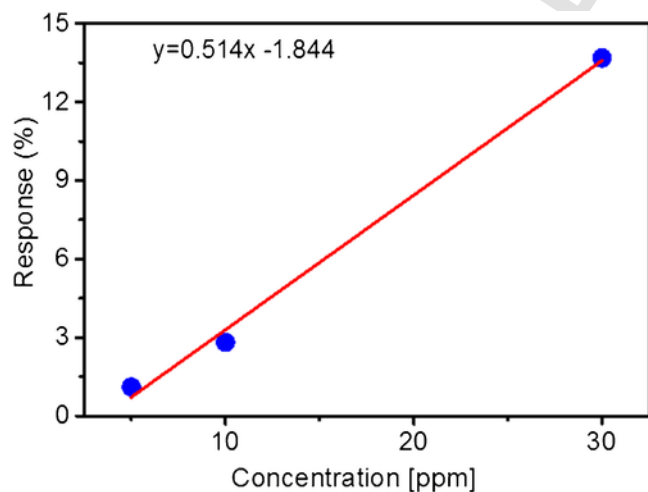


Fig. 9. Calibration curve for acetaldehyde detection.

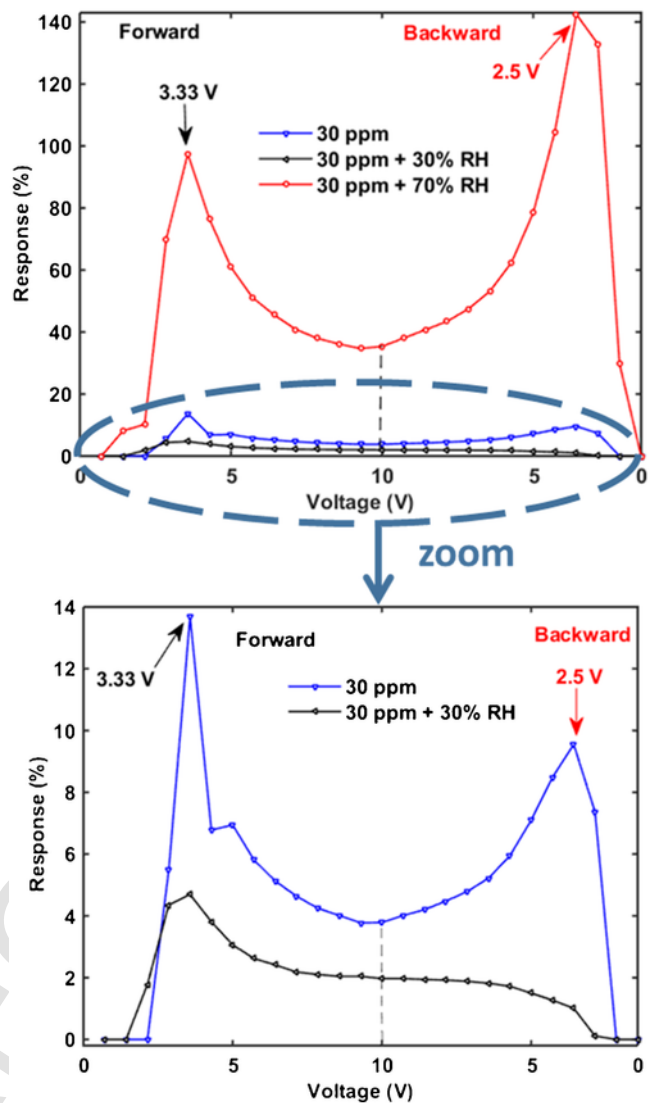


Fig. 10. Response curves to 30 ppm of acetaldehyde obtained under different RH levels.

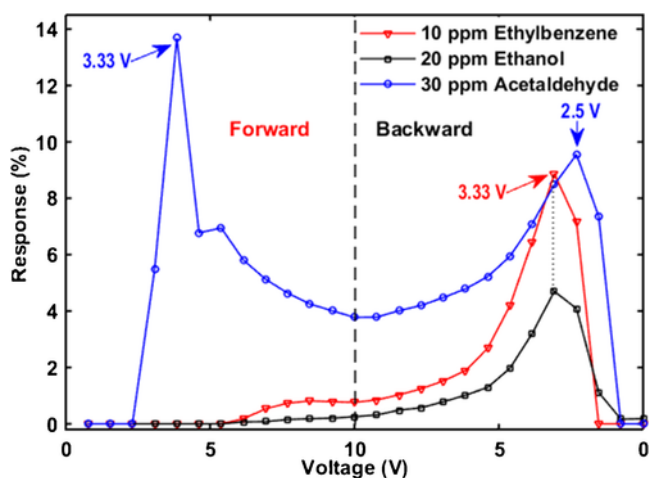


Fig. 11. Response curves obtained from sensor's exposure to different VOCs.

sensing devices based on these nano-assemblies showed Schottky-diode behaviour. We believe this is the first observation of Schottky-diodes fabricated from nanomaterials based on metallic nanoparticles. Gas sensing experiments demonstrated that these devices were suitable for detection of volatile organic compounds. Furthermore, we introduced a novel method to analyse the response of a Schottky-diode chemical gas sensor, whose response is calculated at each voltage as the relative current change produced by sensor's exposure to the VOC with regard to the current in synthetic dry air. This measurement technique offers novel features for fingerprinting VOC detection.

### Acknowledgments

The research leading to these results has been partially funded by the Spanish Ministry for Economy and Competitiveness - MINECO (Grant Number TEC2012-32420). Work at Uppsala University was supported by the European Research Council under the European Community's Seventh Framework Program (FP7/2007–2013)/ERC Grant Agreement No. 267234 ("GRINDOOR"). R.I. holds a Ramón y Cajal fellowship from MINECO. R.I. acknowledges a mobility fellowship from the Agency for Management of University and Research Grants (AGAUR), Catalonia Region, Spain. E.L. was awarded the ICREA Academia Award in the 2012 Edition.

### Appendix A. Supplementary data

Supplementary data associated with this article can be found, in the online version, at <http://dx.doi.org/10.1016/j.snb.2016.07.182>.

### References

- [1] U. Tisch, H. Haick, Nanomaterials for cross-reactive sensor arrays, *MRS Bull.* 35 (2010) 797–803.
- [2] N. Babajani, P. Kowalzik, R. Waser, M. Homberger, C. Kaulen, U. Simon, S. Karthäuser, Electrical characterization of 4-mercaptophenylamine-capped nanoparticles in a heterometallic nanoelectrode gap, *J. Phys. Chem. C* 117 (2013) 22002–22009.
- [3] J.C. Azcárate, G. Corthey, E. Pensa, C. Vericat, M.H. Fonticelli, R.C. Salvarezza, P. Carro, Understanding the surface chemistry of thiolate-protected metallic nanoparticles, *J. Phys. Chem. Lett.* 4 (2013) 3127–3138.
- [4] H. Haick, Chemical sensors based on molecularly modified metallic nanoparticles, *J. Phys. D: Appl. Phys.* 40 (2007) 7173.
- [5] G. Shuster, S. Baltianski, Y. Tsur, H. Haick, Utility of resistance and capacitance response in sensors based on monolayer-capped metal nanoparticles, *J. Phys. Chem. Lett.* 2 (2011) 1912–1916.
- [6] B. Raguse, C.S. Barton, K.-H. Muller, E. Chow, L. Wiczorek, Gold nanoparticle chemiresistor sensors in aqueous solution: comparison of hydrophobic and hydrophilic nanoparticle films, *J. Phys. Chem. C* 113 (2009) 15390–15397.
- [7] N. Peled, R. Ionescu, P. Nol, O. Barash, M. McCollum, K. VerCauteren, M. Koslow, R. Stahl, J. Rhyhan, H. Haick, Detection of volatile organic compounds in cattle naturally infected with *Mycobacterium bovis*, *Sens. Actuators B: Chem.* 171–172 (2012) 588–594.
- [8] M. Brust, J. Fink, D. Bethell, D. Schiffrin, C. Kiely, Synthesis and reactions of functionalised gold nanoparticles, *J. Chem. Soc. Chem. Commun.* 16 (1995) 1655–1656.
- [9] M.A. Correa-Duarte, N. Pazos Perez, L. Guerrini, V. Giannini, R.A. Alvarez-Puebla, Boosting the quantitative inorganic surface-enhanced Raman scattering sensing to the limit: the case of nitrite/nitrate detection, *J. Phys. Chem. Lett.* 6 (2015) 868–874.
- [10] M.D. Malinsky, K.L. Kelly, G.C. Schatz, R.P. Van Duyne, Chain length dependence and sensing capabilities of the localized surface plasmon resonance of silver nanoparticles chemically modified with alkanethiol self-assembled monolayers, *J. Am. Chem. Soc.* 123 (2001) 1471–1482.
- [11] J. Hu, J. Zhang, F. Liu, K. Kittredge, J.K. Whitesell, M.A. Fox, Competitive photochemical reactivity in a self-assembled monolayer on a colloidal gold cluster, *J. Am. Chem. Soc.* 123 (2001) 1464–1470.
- [12] C. Granqvist, R. Buhrman, Ultrafine metal particles, *J. Appl. Phys.* 47 (1976) 2200–2219.
- [13] J. Ederth, L. Kish, E. Olsson, C. Granqvist, Temperature dependent electrical resistivity in nanocrystalline gold films made by advanced gas deposition, *J. Appl. Phys.* 88 (2000) 6578–6582.
- [14] J. Ederth, L. Kish, E. Olsson, C. Granqvist, In situ electrical transport during isothermal annealing of nanocrystalline gold films, *J. Appl. Phys.* 91 (2002) 1529–1535.
- [15] S. Malola, H. Hakkinen, Electronic structure and bonding of icosahedral core-shell gold-silver nanoalloy clusters Au<sub>144-x</sub>Ag<sub>x</sub> (SR) 60, *J. Phys. Chem. Lett.* 2 (2011) 2316–2321.
- [16] G. Peng, U. Tisch, O. Adams, M. Hakim, N. Shehata, Y.Y. Broza, S. Billan, R. Abdah-Bortnyak, A. Kuten, H. Haick, Diagnosing lung cancer in exhaled breath using gold nanoparticles, *Nat. Nanotechnol.* 4 (2009) 669–673.
- [17] Z.q. Xu, Y.Y. Broza, R. Ionsecu, U. Tisch, L. Ding, H. Liu, Q. Song, Y.y. Pan, F.x. Xiong, K.s. Gu, G.p. Sun, Z.d. Chen, M. Leja, H. Haick, A nanomaterial-based breath test for distinguishing gastric cancer from benign gastric conditions, *Br. J. Cancer* 108 (2013) 941–950.
- [18] W.L. Armarego, C.L.L. Chai, Purification of Laboratory Chemicals, 7th ed., Butterworth-Heinemann, Elsevier, Oxford, 2013.
- [19] S.W. Han, Y. Kim, K. Kim, Dodecanethiol-derivatized Au/Ag bimetallic nanoparticles: TEM, UV/VIS, XPS, and FTIR analysis, *J. Colloid Interface Sci.* 208 (1998) 272–278.
- [20] B.L. Dokić, B. Blanuša, Power electronics. Converters and regulators, Diodes and Transistors, Springer, 201543–141, Chapter 2.
- [21] E. Miranda, D. Jiménez, A. Tsurumaki-Fukuchi, J. Blasco, H. Yamada, J. Suñé, A. Sawa, Modeling of hysteretic Schottky diode-like conduction in Pr<sub>2</sub>BiFeO<sub>3</sub>/SrRuO<sub>3</sub> switches, *Appl. Phys. Lett.* 105 (2014) 082904.
- [22] P. Pang, Z. Guo, Q. Cai, Humidity effect on the monolayer-protected gold nanoparticles coated chemiresistor sensor for VOCs analysis, *Talanta* 65 (2005) 1343–1348.
- [23] P. Pang, J. Guo, S. Wu, Q. Cai, Humidity effect on the dithiol-linked gold nanoparticles interfaced chemiresistor sensor for VOCs analysis, *Sens. Actuators B: Chem.* 114 (2006) 799–803.

**Radu Ionescu** is 'Romón y Cajal' Senior Researcher in the group of Microsystems and Nanotechnology for Chemical Analysis (MINOS), at the Department of Electronics, Electrical and Automatic Engineering, Rovira i Virgili University, Tarragona, Spain. He received his degree in Electrical Power Engineering from the Polytechnic University of Bucharest, Romania, in 1998, and his Ph.D. degree in Electronics Engineering from the Polytechnic University of Catalonia, Barcelona, Spain, in 2003. Previously, Dr. Radu Ionescu was post-doctoral researcher at Rovira i Virgili University, Tarragona, Spain, experienced researcher (FP6 Marie Curie Transfer of Knowledge Actions) at Mediterranean University of Reggio Calabria, Italy, and EC Senior Researcher at the Technion – Israel Institute of Technology, Haifa, Israel. Dr. Radu Ionescu's research focuses on the development of chemical gas sensors for VOCs detection and diseases diagnosis through volatile samples analysis. Dr. Ionescu is the Coordinator of the EU funded H2020-MSCA-RISE-2014 project "Development of a non-invasive breath test for early diagnosis of tropical diseases" – TROPSENSE. In 2015, Dr. Ionescu organised the Symposium "Approaches and Nanotechnologies for Volatolomics" ([www.volasy.com](http://www.volasy.com)).

**Umut Cindemir** received the B.S. and M.S. degrees from the Electrical and Electronics Engineering Department, Boğaziçi University, Istanbul, Turkey, in 2009 and 2011, respectively. Currently, he is working toward the Ph.D. degree as a student in the Engineering Sciences Department, Uppsala University, Uppsala, Sweden. His research interests include design, fabrication, and characterization of micro-mechanical systems (MEMS) and integration of MEMS structures with electronic circuits. His current field of study is to design gas sensors for indoor air monitoring applications

**Tesfalem G. Welearegay** received his B.Sc in Applied Chemistry from Debub University in 2006, and the M.Sc degree in Physical Chemistry from Addis Abab University in 2009 (Ethiopia). He was also awarded a M.Sc in Nanoscience and Nanotechnology from Rovira i Virgili University in 2013 (Spain). He is now doing his PhD research at the Department of Electronic, Electrical, and Automatic Engineering, Rovira i Virgili University (Spain) since 2014. His major area of research includes fabrication, characterization and functionalization of metal nanoparticles based sensors for VOCs detection, as well as fabrication of microsensor platforms based on functionalized metal oxides for gas sensors.

**Raul Calavia** is a research technician at the Department of Electronics Engineering of Universitat Rovira i Virgili in Tarragona (Spain). He finished his Ph.D. in 2012 at Universitat Rovira i Virgili. His research is centred on nanostructured metal oxide films obtained by anodisation for gas sensing and biological applications.

**Zouhair Haddi** received his joint (Cotutelle) Ph.D. in Electronics, artificial intelligence, and Engineering from the Moulay Ismaïl University (Meknes, Morocco) and Université de Lyon (France) in 2013. He is currently a Postdoc at Aix-Marseille University. His research interests include chemical gas sensors, nanomaterials, and pattern recognition methods applied to electronic sensing systems for food and medical purposes.

**Zareh Topalian** is Postdoctoral Researcher in the Department of Solid State Physics, the Ångström Laboratory, Uppsala University, Sweden. He got his PhD diploma in Solid State Physics from the

same University in 2011. His main research interests focus on solid state gas sensors and self-cleaning surfaces,

**Claes-Göran Granqvist** is Senior Professor in Solid State Physics at the Ångström Laboratory of Uppsala University, Sweden. His current research interests include materials science for solar energy and energy efficiency, particular regarding benign indoor environments, and include electrochromics, thermochromics, air quality sensing, and air cleaning by photocatalysis. The work is summarised in numerous publications, books, and proceedings volumes. Granqvist is a member of several Academies and Learned Societies, including the Royal Swedish Academy of Sciences and the Royal Swedish Academy of Engineering Sciences. He has received several recognitions and prizes, most recently the 2015 Jan Czochralski Award.

**Eduard Llobet** is a full professor at the Department of Electronic Engineering of the Universitat Rovira i Virgili in Tarragona (Spain). He was awarded a Ph.D. in 1997 from the Technical University of Catalonia (Barcelona) and then joined the Gas Sensor Lab (UWarwick, UK) for a one-year postdoc. From 2010 to 2014 he was Director of the Research Centre on Engineering of Materials and micro/nano Systems. He is currently addressing the fabrication of sensor arrays employing low-dimensional metal oxides and carbon nanomaterials. Cost-effective and industrially scalable methods are considered for bottom-up integration in MEMS or flexible platforms. The applications sought are (i) sensitive and selective gas microsensors for environmental monitoring, medicine or safety and (ii) heterogeneous catalysis. He got the ICREA Academia Award in the 2012 Edition.